

## Sustained Activation of Mitogen-Activated Protein Kinases and Activator Protein 1 by the Hepatitis B Virus X Protein in Mouse Hepatocytes In Vivo

RUCHIKA NIJHARA,<sup>1</sup> SIDDHARTHA S. JANA,<sup>1</sup> SHYAMAL K. GOSWAMI,<sup>2</sup> AJAY RANA,<sup>3</sup>  
SUBEER S. MAJUMDAR,<sup>4</sup> VIJAY KUMAR,<sup>5</sup> AND DEBI P. SARKAR<sup>1\*</sup>

*Department of Biochemistry, University of Delhi South Campus, New Delhi-110021,<sup>1</sup> and School of Life Sciences, Jawaharlal Nehru University,<sup>2</sup> National Institute of Immunology, Aruna Asaf Ali Marg,<sup>4</sup> and Virology Group, International Centre for Genetic Engineering and Biotechnology, Aruna Asaf Ali Marg,<sup>5</sup> New Delhi-110067, India, and Division of Molecular Cardiology, Texas A&M University System Health Science Center, Temple, Texas 76504<sup>3</sup>*

Received 26 March 2001/Accepted 30 July 2001

**Transcriptional activation of diverse cellular genes by the X protein (HBx) of hepatitis B virus (HBV) has been suggested as one of the mechanisms for HBV-associated hepatocellular carcinoma. However, such functions of HBx have been studied using transformed cells in culture and have not been examined in the normal adult hepatocytes, a natural host of HBV. Using an efficient hepatocyte-specific virus-based gene delivery system developed in our laboratory earlier, we studied the HBx action in vivo. We demonstrate that following virosome-mediated delivery of HBx DNA, a large population (>50%) of hepatocytes express the HBx protein in a dose-dependent manner, which induces a significant increase in the activity of extracellular signal-regulated kinases (ERKs) in the livers of HBx-transfected mice. Inhibition of HBx-induced ERK activation following intravenous administration of PD98059, a mitogen-activated protein kinase kinase kinase (MEK) inhibitor, confirmed the requirement for MEK in the activation of ERKs by HBx. Induction of ERK activity by HBx was sustained for up to 30 days. Interestingly, sustained activation of c-Jun N-terminal kinases (JNKs) for up to 30 days was also noted. Such constitutive ERK and JNK activation as a consequence of continued HBx expression also led to sustained stimulation of further downstream events, such as increased levels of c-Jun and c-Fos proteins along with the persistent induction of activator protein 1 binding activity. Taken together, our data suggest a critical role of these molecules in HBx-mediated cell transformation.**

Hepatitis B virus (HBV), a prototype member of mammalian hepadnaviruses, predominantly infects host hepatocytes and causes a spectrum of pathological processes, ranging from inapparent infection to the later development of primary liver cancer (61). The molecular mechanism underlying HBV-mediated carcinogenesis is incompletely understood. Nonetheless, it is postulated that it does not involve direct insertional activation of proto-oncogenes, although modulation of cellular gene expression by transmechanisms might play a significant role (14, 19). The HBV-encoded X gene product (HBx) can induce transformation of cultured cells and tumors in certain transgenic mice, and the HBx gene is integrated in the host chromosome in many tumors despite the absence of other HBV genes (14, 39, 48). These observations shed light on the mechanism of HBV-associated carcinogenesis and suggest the relevance of the X open reading frame to the development of hepatocellular carcinoma (HCC). Chromosomal DNA from HBV-associated tumors often possesses X sequences, which, in spite of being truncated, retain their transactivating function and suggest the importance of HBx-mediated transactivation in carcinogenesis (48). However, little is known about the exact role of HBx in tumorigenesis. HBx deregulates cell cycle

checkpoints (10) and stimulates DNA synthesis, leading to the proliferation of quiescent fibroblasts (33). Importantly, HBx (16.5 kDa) is a moderate but broad-acting transcriptional transactivator and activates a variety of cellular and viral genes, including proto-oncogenes, such as c-myc, c-Fos, and c-Jun, thus regulating in turn many host functions, such as transcription, cell cycle progression, proliferation, apoptosis, and DNA repair (2, 4, 32). However, HBx does not bind to DNA directly, and transactivation involves direct protein-protein interactions between HBx, the cellular transcription machinery, and other regulatory proteins (48). HBx influences transcription directly by interacting with the basal transcriptional apparatus and bZip transcription factors (2). In the cytoplasm, which is its predominant site of localization (18, 48), HBx activates transcription indirectly by modulating signal transduction pathways, particularly protein kinase C (PKC) (27), JAK/STAT (40), Src (30), and Ras signaling (9, 11, 36). Transcriptional deregulation has thus been implicated as the possible mechanism by which HBx mediates hepatocyte transformation.

Activation of the Ras-Raf-mitogen-activated protein kinase (MAPK) cascade is necessary for cell growth and proliferation (41, 55). MAPKs serve as convergence points in intracellular signal transducing pathways and couple cytoplasmic signals to the gene expression program (34). Constitutively active mutants in this pathway exhibit enhanced kinase activity, leading to the transformed phenotypes (15). The conditions that influence this pathway in the intact liver are emerging. Recent

\* Corresponding author. Mailing address: Department of Biochemistry, University of Delhi South Campus, Benito Juarez Road, New Delhi 110021, India. Phone: 91-11-6881967. Fax: 91-11-6885270 or 91-11-6886427. E-mail: sarkar@del3.vsnl.net.in or dpsarkar@hotmail.com.

studies demonstrate the activation of MAPKs under both hormonal (e.g., epidermal growth factor and hepatocyte growth factor) and nonhormonal (e.g., sodium orthovanadate and partial hepatectomy) stimulation of quiescent hepatocytes in the intact liver (51, 59). Constitutive activation of the MAPK signaling pathway has also been observed in a large number of tumors (23, 24, 42, 57). Since many physiological and etiological processes require extracellular signal-regulated kinase (ERK) activation, it is intriguing to examine its role in the HBx-induced signal transduction activity with a view to comprehend its possible relevance in carcinogenesis. Notably, all the evidence provided on HBx-induced transactivation of cellular signaling pathways has been obtained with transformed cell lines in culture and reflects conditions that are nonnative to the environment in which HBx is expressed during infection with HBV. In addition, a number of studies have emphasized the limited value of *in vitro* systems for the analysis of HBx protein function and underscored the importance of *in vivo* studies on HBx (54, 60). However, no evidence exists from whole animals in support of HBx-induced modulation of signal transduction pathways.

Exploiting the membrane-fusogenic ability of Sendai virus F glycoprotein and the high affinity of the terminal  $\beta$ -galactose-containing ligand (present on F glycoprotein) for the asialoglycoprotein receptor on the hepatocyte surface, we have developed an efficient virus-based delivery system (F-virosomes) (55a) to transfer foreign genes to mouse hepatocytes *in vivo* (6, 7, 53). Using this system, we have now introduced the HBx gene into the whole animal and examined the effect of hepatocyte-expressed HBx protein on signaling cascades. We demonstrate for the first time that HBx expression *in vivo* induces MAPKs and activator protein 1 (AP-1) activation persistently, and we suggest that these changes precede carcinoma formation.

#### MATERIALS AND METHODS

**Expression vector of HBx.** The construction of a eukaryotic expression vector for HBx has been described earlier (37). Briefly, the HBx gene was amplified as a 481-bp DNA fragment by PCR using the full-length HBV template (adw subtype) and the following oligonucleotide primers: forward, 5'-CGGAATTCATGGCTGCTAGGCTGT-3', and reverse, 5'-CGGAATTCCTTAGGCAGAGGTGAAAAAG-3'. Finally, a 471-bp *EcoRI* fragment of the HBx gene was cloned into pSG5 (Stratagene) under the control of the SV40 promoter. All plasmids were isolated using the Qiagen Megaprep kit.

**Intravenous injection of DNA-loaded virosomes, insulin, and PD98059 into BALB/c mice.** The F-virosomes containing HBx DNA were prepared following our standardized protocol (53). In brief, 75  $\mu$ g of each plasmid was incubated with a detergent-solubilized fraction of Sendai virus containing its envelope devoid of hemagglutinin-neuraminidase protein. Finally, F-virosomes containing the DNA were prepared by stepwise removal of detergent by using SM2 Biobeads (Bio-Rad). The membrane fusion-mediated cytosolic delivery of its contents was evaluated by published protocols (6, 7) prior to their injection to animals. Twelve-week-old female BALB/c mice ( $\approx$ 18 g) were injected intravenously (i.v.) in the tail vein with 2  $\mu$ g of DNA loaded in F-virosomes. Twenty micrograms of insulin (Sigma) in phosphate-buffered saline (PBS) was injected i.v. into mice 1 h prior to sacrifice. i.v. administration of PBS containing 75  $\mu$ M PD98059 (New England Biolabs) in 0.37% dimethyl sulfoxide was done 5 h before the sacrifice of HBx- and insulin-injected mice. Injection of PBS alone (mock injection), pSG5 vector DNA-loaded F virosomes, and PBS with 0.37% dimethyl sulfoxide served as appropriate negative controls. Throughout the experiments, these animals were maintained under constant room temperature with a 12:12-h light-dark cycle under specific pathogen-free conditions and were offered food and water *ad libitum*, and experiments were carried out in accordance to Delhi University laws and regulations. At various time intervals, animals were sacrificed and livers were processed as described below. A portion of each

liver was kept frozen for both the isolation of total RNA and the preparation of nuclear extracts. All experiments were independently repeated at least three times.

**Histological and immunohistochemical methods.** A portion of each liver from injected mice was immediately fixed in Bouin's fixative and dehydrated through graded alcohol and xylene followed by embedding in paraffin wax. Paraffin-embedded tissues were cut into 5- $\mu$ m sections, deparaffinized, and rehydrated. For immunostaining, sections were washed in PBS for 10 min and blocked with 3% bovine serum albumin in PBS for an hour at 37°C. Subsequently, sections were incubated with an HBx-specific monoclonal antibody (B-8/2/8) (37) for an hour at 37°C. After three washes with PBS, sections were incubated with alkaline phosphatase-conjugated goat anti-mouse immunoglobulin G (IgG) (Sigma) at 37°C for an hour. All antibody dilutions were made in 1.5% bovine serum albumin in PBS. Following extensive washes with PBS, color development was demonstrated with the addition of Fast Red solution (DAKO, Glostrup, Denmark). Finally, the slides were counterstained with Mayer's hematoxylin, washed in distilled water, and mounted in glycerol. The specificity of immunostaining was verified by the use of PBS in place of primary antibody (data not shown). The sections were examined using light microscopy and photographed (magnification,  $\times$ 100).

**Hepatocyte isolation from liver biopsy and HBx gene expression.** Parenchymal cell (hepatocytes) separation was carried out as described in an earlier report by members of our group (53). To summarize, perfused livers were washed and treated with 0.05% collagenase (GIBCO BRL). The resulting cell suspension was filtered through a nylon mesh, and the filtrate was centrifuged to obtain a pellet containing hepatocytes. Residual blood cells were separated from the hepatocyte population by a modification of a method described earlier (43). Finally, hepatocytes free of detectable red blood cells were collected.

(i) **HBx protein detection in total hepatocyte lysates.** After 2 days of injection of HBx DNA-loaded F-virosomes, hepatocytes were isolated, directly lysed in Laemmli sample buffer, and analyzed by sodium dodecyl sulfate–15% polyacrylamide gel electrophoresis (SDS–15% PAGE) followed by immunoblotting with an HBx-specific monoclonal antibody (B-8/2/8) (37). Protein bands were visualized using the enhanced chemiluminescence (ECL) system (Santa Cruz Biotechnology). pET-X-expressing X protein in *Escherichia coli* (rec-HBx) after isopropyl- $\beta$ -D-thiogalactopyranoside induction was used as a position marker for X protein during immunoblotting (25).

(ii) **RT-PCR amplification of HBx gene-specific transcript.** Total hepatic RNA from various mice was isolated using the TRIZOL reagent (GIBCO BRL). The primer set designed for HBx included the following: sense, 5'-CGGAATTCATATGCTCCCCGCTGTGCCTTC-3'; antisense, 5'-CGGAATTCGGATCCTTATTTGTGC CTACAGCTCCTAA-3'. DNase I (GIBCO BRL)-treated RNA was reverse transcribed using Superscript RNase H<sup>-</sup> reverse transcriptase (RT) (GIBCO BRL) and gene-specific antisense primer as per the manufacturer's protocol. PCR amplification (35 cycles) of the RT product was performed using high-fidelity Platinum *Taq* DNA polymerase (GIBCO BRL) with a cycling profile of 94°C for 45 s, 62°C for 45 s (or 55°C for 45 s in the case of  $\beta$ -actin primers; Stratagene), 72°C for 1 min, and a final extension at 72°C for 10 min. A specific amplified product of 270 bp of the HBx gene was visualized by ethidium bromide staining on a 1.5% agarose gel. As a control,  $\beta$ -actin mRNA was also amplified by RT-PCR for each sample, and a product of 650 bp was obtained. Southern hybridization was performed to further confirm the specificity of the RT-PCR product using a <sup>32</sup>P-labeled HBx DNA fragment as the probe.

**Kinase assay.** The ERK assay was performed following a published protocol (9) with some changes. In brief, hepatocytes isolated from mouse livers were lysed in a lysis buffer (20 mM Tris-HCl, pH 7.5, containing 150 mM NaCl, 1.0% Triton X-100, 10% glycerol, 1 mM dithiothreitol, 1 mM NaF, 1 mM Na<sub>3</sub>VO<sub>4</sub>, 20 mM *para*-nitrophenyl phosphate, 50 mM  $\beta$ -glycerol phosphate, 1 mM EGTA, 2 mM PMSE, 1.5 mM MgCl<sub>2</sub>, and 20  $\mu$ g each of aprotinin and leupeptin [Sigma]/ml along with Complete protease inhibitor cocktail [Roche]). Protein concentration in the lysates was measured by the Bradford assay. Assessment of ERK/MAPK activity was carried out by *in vitro* phosphorylation of exogenous substrate myelin basic protein (MBP) (GIBCO BRL). For each sample, 5  $\mu$ g of protein lysate was used in a reaction containing 5  $\mu$ g of MBP in kinase buffer (20 mM Tris-HCl [pH 7.5], 40 mM MgCl<sub>2</sub>, 10  $\mu$ M ATP [Sigma]) and 2  $\mu$ Ci of [ $\gamma$ -<sup>32</sup>P]ATP (Amersham Pharmacia Biotech) and incubated for 30 min at 30°C. The reaction was stopped by the addition of Laemmli sample buffer and resolved on SDS–15% PAGE. The upper half of the gel was used for Western analysis with anti-ERK antibody (Santa Cruz Biotechnology) using the ECL detection system. The lower half of the gel containing MBP protein was dried and exposed to X-ray films. Coomassie blue (CB) staining was done with the dried blot to check for equal amounts of MBP present in each reaction. The stained MBP

bands were excised, and incorporated radioactivity was measured by liquid scintillation counting for calculating fold activation.

**Detection of phosphorylated ERK and JNK by immunoblotting.** The level of active forms of ERK (P-ERK) and c-Jun N-terminal MAPK (P-JNK) in the hepatocyte cell lysates (5  $\mu$ g each) were examined separately by Western blotting with anti-phospho-p44/42 MAPK antibody and Phospho Plus SAPK/JNK Antibody (Cell Signaling Technology), respectively. Respective blots were stripped and reprobed with anti-ERK antibody and anti-JNK antibody.

**Preparation of nuclear extracts and gel mobility shift assay.** Nuclear extracts from each liver lobe and HepG2 cells were prepared as described by Lassar et al. (38). Corresponding cytosolic extracts obtained were used for immunoprecipitation of the HBx protein by anti-HBx antibody. Electrophoretic mobility shift assays (EMSA) were carried out essentially following a published protocol (11). The synthetic oligonucleotides used as a probe or competitor DNA in this assay consisted of double-stranded TRE sequence (Promega). Binding reactions with 36  $\mu$ g of liver nuclear extracts and 6  $\mu$ g of HepG2 cell extracts were carried out for 60 min at 4°C followed by incubation for 5 min at 25°C using 10,000 cpm of <sup>32</sup>P-labeled probe and 1  $\mu$ g of poly(dI · dC) (Sigma). Competition binding experiments were performed with unlabeled oligonucleotide in excess. The reaction mixture was resolved on a 4% nondenaturing polyacrylamide gel, dried, and visualized by autoradiography or PhosphorImaging analysis. For antibody (supershift) studies, 4  $\mu$ g of antiserum (Santa Cruz Biotechnology) to either c-Jun or c-Fos was added after completion of the binding reaction and incubated at 28°C for 20 min. Seventy micrograms of the same nuclear extracts were subjected to Western blotting using specific antibody as described for the supershift assay and visualized by the ECL detection system.

## RESULTS

**Expression of HBx gene in mouse liver following F-virosome-mediated delivery.** To test exogenous HBx gene expression in mouse liver, hepatocytes isolated 2 days after injection of loaded virosomes were analyzed by Western blotting using the monoclonal antibody B-8/2/8 (Fig. 1a). A band corresponding to the 16.5-kDa protein (lane 4) similar in mobility to a recombinant X protein (rec-HBx; lane 5) (25) was detected only in mouse hepatocytes injected with the HBx gene, confirming both the expression and structural integrity of the HBx protein in hepatocytes. Mock injection, vector-loaded virosomes, and free DNA (lanes 1 to 3) served as negative controls. Total RNA was isolated from the same liver biopsies and examined for HBx-specific mRNA through RT-PCR analysis (Fig. 1b). As expected, amplified product of HBx-specific transcript was obtained (lane 4, upper and middle panels), while no corresponding band was seen in any of the negative controls (lanes 1 to 3). Equal loading of RNA and its integrity were confirmed by RT-PCR analysis of  $\beta$ -actin mRNA (Fig. 1b, lower panel). In a separate experiment, the hepatocyte-specific HBx gene delivery was confirmed by the absence of any detectable level of protein or RNA in nonparenchymal cells and other tissues, such as those from heart, lungs, kidneys, brain, spleen, and skeletal muscle (data not shown). Absence of any detectable protein or RT-PCR signal from administration of free HBx DNA demonstrated the efficiency of this delivery mode. Furthermore, the presence of the HBx protein in individual hepatocytes was demonstrated by immunohistochemical analysis with the fixed liver tissue sections (Fig. 1c). Immunostaining of liver sections from experimental mice (2 days postinjection) using the monoclonal antibody B-8/2/8 showed that as much as 50 to 70% of the hepatocytes were expressing the HBx protein following introduction of 2  $\mu$ g of HBx DNA entrapped in virosomes (panel 1). Importantly, HBx expression was exclusive for the hepatocytes, in conformity with the cell-specific nature of the virosomal delivery system in vivo. However, we found heterogeneity in terms of both distribution of

HBx-expressing hepatocytes and the relative level of HBx per cell over the entire liver (data not shown). We anticipate that such a phenomenon may be attributed to differential delivery of the HBx gene by virosomes. Even more impressive was the observation that livers receiving 5  $\mu$ g of the HBx plasmid through virosomes showed a nearly complete transfection with intense staining. No immunostaining was detected in the liver sections from vector-injected control mice (panels 2 and 4). This observation indicates that by augmenting the dose of delivered HBx gene, both the number of hepatocytes getting transfected and the abundance of the HBx protein per cell can be increased. Overall, these results establish the virosome-mediated delivery of the HBx gene specifically to the hepatocytes in vivo, as confirmed both by expression of the protein and its transcript. Considering its sensitivity, only RT-PCR analysis has been utilized throughout our experiments as a clear reflection of HBx gene expression. It is noteworthy that all the animals remained healthy and active during the entire study.

**Activation of ERKs by HBx in mouse hepatocytes.** Following successful expression of HBx in mouse hepatocytes, we next evaluated its transactivation potential in activating mitogenic signaling pathways in vivo. Hepatocyte lysates prepared from HBx-, vector-, and insulin-injected mice were tested for the phosphorylation of ERK1 and ERK2 (ERK1/2). As shown in Fig. 2a (upper panel), HBx-expressing hepatocyte lysates (lane 3) showed a significant increase of P-ERK levels over the controls (lanes 1 and 2), similar to that in insulin-induced cell lysates (positive control, lane 4). Nonetheless, the extent of expression of ERK1/2 was not altered significantly in any of the samples (lower panel). Note that although the presence of both ERK1/2 forms of MAPK were detected in all the samples tested, the two distinguishable forms of the corresponding P-ERKs were not readily apparent, perhaps owing to the comigration after phosphorylation. In addition, the functional activity of phosphorylated ERK proteins in these extracts was defined by an in vitro kinase assay using MBP as a specific substrate. In agreement with the elevated P-ERK activity, a four- and fivefold elevation in MBP phosphorylation were observed in lysates from HBx and insulin-injected animals, respectively (Fig. 2b, upper panel, lanes 3 and 4, and Fig. 2c). Equal protein loading in all blots was verified by Ponceau S red staining (data not shown). Insulin, a well-known stimulator of ERK in Ras-Raf-MAPK cascades (13), alluded to the involvement of this pathway in HBx-induced ERK up-regulation in vivo. These observations established the potential of the HBx protein to stimulate the ERK cascade in vivo.

**Dose-dependent activation of ERKs by HBx.** We determined the kinetics of ERK activation by HBx and determined the optimum conditions under which functional analysis of HBx could be done. Following injection of increasing amounts of HBx DNA through virosomes, there was a dose-dependent enhancement of both phosphorylation (Fig. 3a, upper panel) and activity (Fig. 3b, upper panel, lanes 2 to 5) of ERK1/2. We observed a fourfold increase in the level of MBP phosphorylation following injection of 1  $\mu$ g of HBx DNA (Fig. 3c). With a further increase in the quantity of DNA, the MBP phosphorylation level increased only moderately and reached a plateau at 5 to 10  $\mu$ g. Steady-state levels of ERK1/2 remained unaltered in all DNA doses studied (Fig. 3a and b, lower panel).

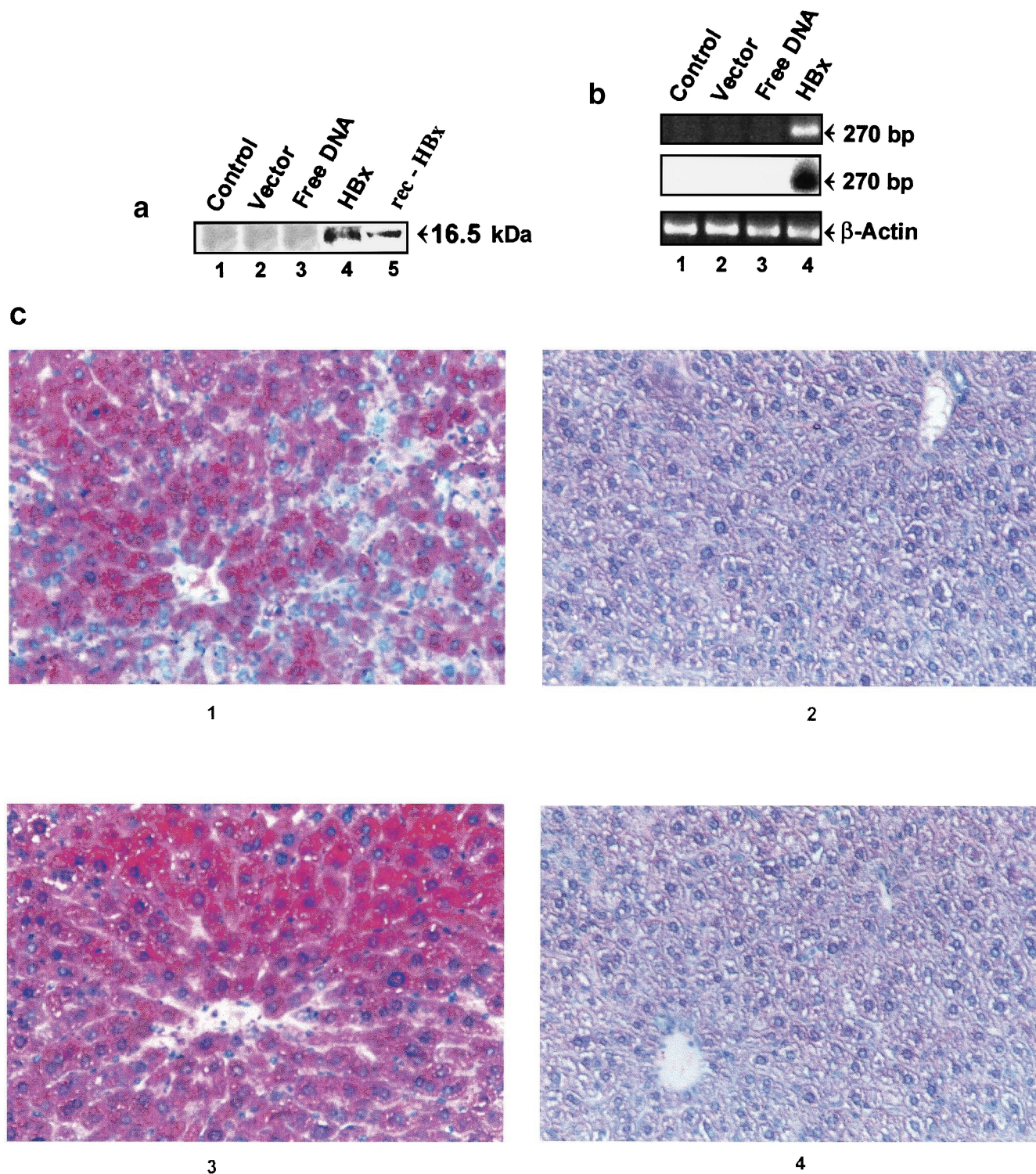


FIG. 1. Exogenous expression of HBx in mouse liver. (a) Immunodetection of HBx protein following virosome-mediated HBx gene delivery to mouse liver. Hepatocyte lysates prepared from mouse livers were resolved by SDS-PAGE and visualized by Western blotting as described in Materials and Methods. (b) Analysis of HBx transcript. Total RNA from a portion of the same liver samples was isolated and analyzed by RT-PCR. The ethidium bromide staining of the PCR product is shown in the upper panel, and Southern hybridization of the same is shown in the middle panel. Corresponding samples were also analyzed for  $\beta$ -actin mRNA (lower panel). (c) Immunohistochemical analysis of HBx protein in fixed liver tissues as a function of DNA dose. Two days postinjection, liver sections from mice injected with 2  $\mu$ g (panel 1) and 5  $\mu$ g (panel 3) of HBx DNA-loaded virosomes were immunostained with an HBx-specific monoclonal antibody (B-8/2/8). Nuclei were visualized (blue color) by counterstaining with hematoxylin. The immunoreactive cells appeared pink with Fast-Red dye. Panels 2 and 4 represent liver sections from mice injected with 2 and 5  $\mu$ g of pSG5 vector DNA-loaded F-virosomes, respectively.

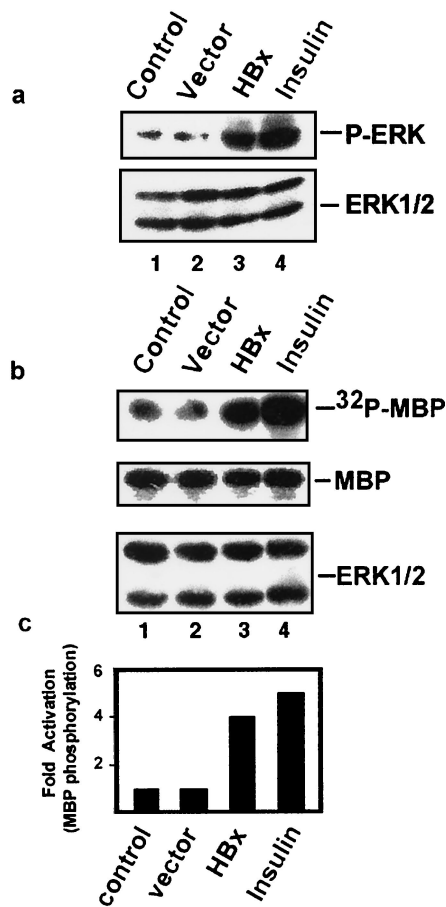


FIG. 2. HBx-mediated activation of ERK in hepatocytes. (a) Determination of P-ERK levels. Hepatocyte lysates were subjected to SDS-PAGE followed by Western blotting using anti-phospho-p44/42 MAPK antibody as described in the text (upper panel). The same blot was stripped and reprobbed with anti-ERK antibody (lower panel). (b) Assessment of functional activity of activated ERKs. The lysates used above were assayed for kinase reactions and resolved by SDS-PAGE. The lower half of the gel was autoradiographed (upper panel), followed by CB staining (middle panel), and the upper half was subjected to Western blotting with ERK antibody (lower panel). (c) Fold activation of MBP phosphorylation. The MBP bands were excised, and radioactivity was measured by liquid scintillation counting.

RT-PCR analysis of the experimental cell extracts was positive for the presence of HBx transgene (Fig. 3d, upper panel). Considering this result, further functional studies of HBx were carried out at the submaximal plasmid quantity of 2  $\mu$ g.

**PD98059 selectively blocks both the phosphorylation and activity of the HBx-induced ERKs.** To ensure whether HBx specifically activates ERK in vivo, we utilized the specific inhibitor of MEK, the kinase that activates ERK1/2 through phosphorylation (1). The effect of this inhibitor on the ERK activation profile in insulin-injected animals was taken as a positive control. In a notable contrast with the case for untreated animals, both HBx-mediated activation of MAPK (P-ERK level) (Fig. 4a) and its activity (fold increase in MBP phosphorylation) (Fig. 4b and c) were effectively abrogated (>66% inhibition) by this MEK inhibitor (Fig. 4b, upper panel, compare lanes 3 and 4). The similar inhibition (>66% inhibition) of the insulin-mediated ERK activation pathway further

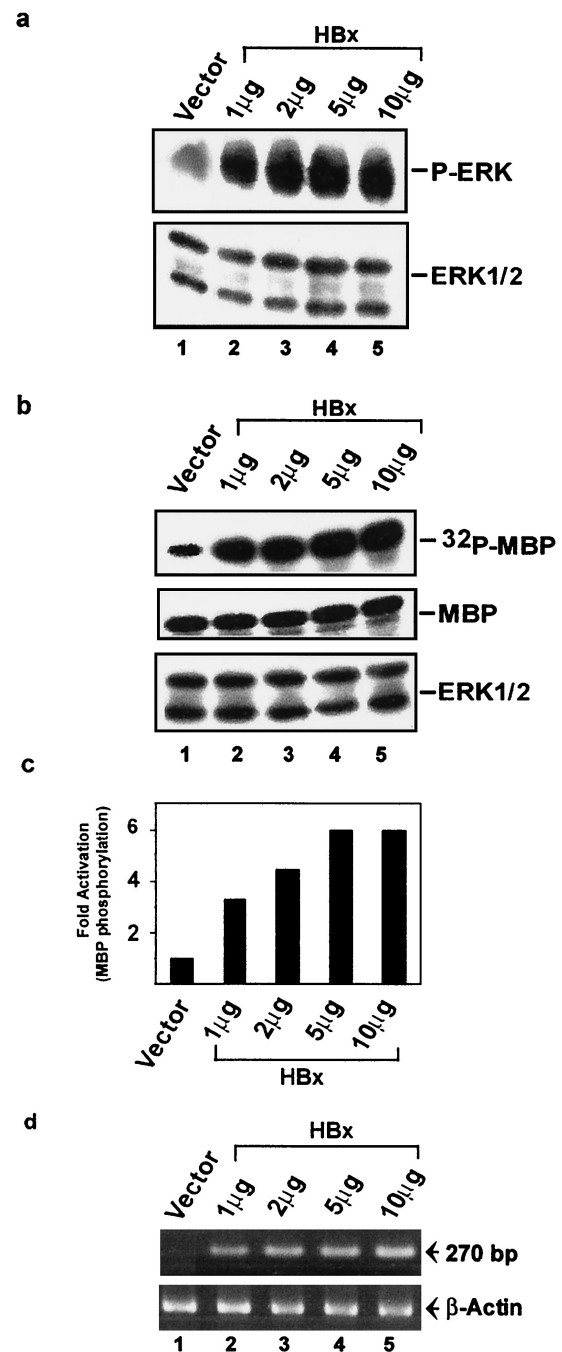


FIG. 3. Dose-dependent activation of ERK by HBx. (a) Equal amounts of hepatocyte lysates were taken for the analysis of P-ERK levels (upper panel) and total ERK levels (lower panel) as described in the legend for Fig. 2. (b) The same lysates were subjected to kinase reactions for evaluation of <sup>32</sup>P-MBP profile (upper panel), CB staining of MBP (middle panel) and total ERK levels (lower panel). (c) Fold activation of MBP phosphorylation. (d) RT-PCR amplification of HBx (upper panel) and  $\beta$ -actin transcripts (lower panel) present in total RNA from each liver specimen was carried out as described in the text.

confirmed the mode of action of PD98059 in vivo (Fig. 4b, upper panel, compare lanes 5 and 6). All liver samples injected with HBx DNA that were tested for MAPK activity exhibited HBx gene expression (Fig. 4d, upper panel, lanes 2 and 3). No significant differences in ERK1/2 protein levels were noted as

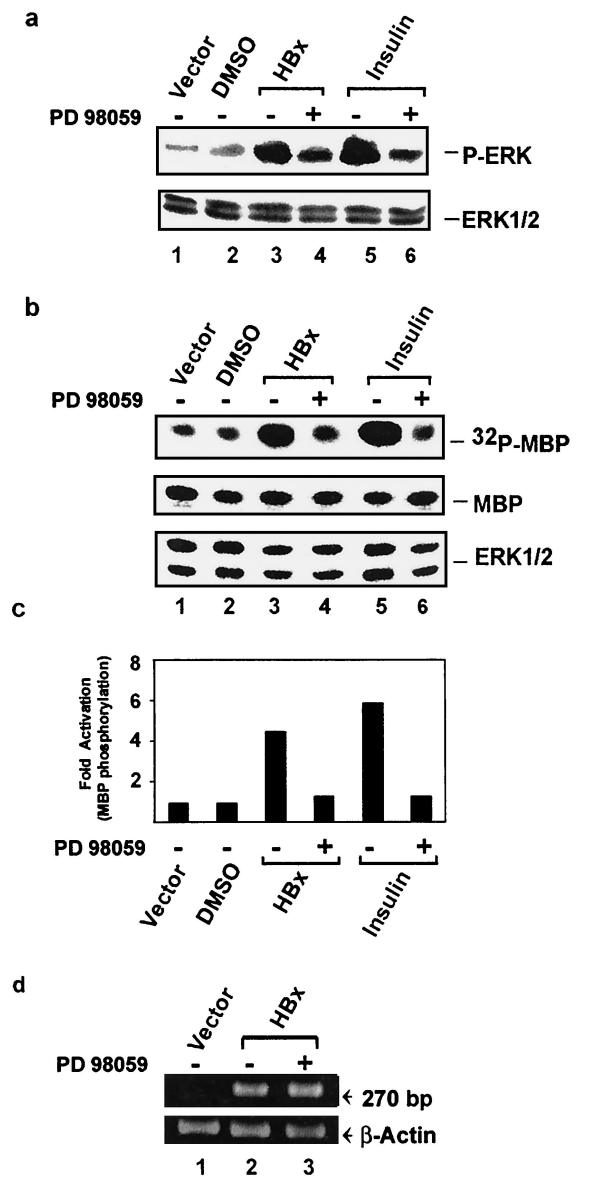


FIG. 4. Effect of PD98059 on ERK activation in vivo. (a) PD98059 inhibits both HBx- and insulin-induced ERK phosphorylation. PD98059 was administered i.v. to two groups of mice, one injected with virosomal HBx DNA and the other with insulin prior to sacrifice, as mentioned in the text. Hepatocyte lysates were evaluated for both ERK1/2 phosphorylation (upper panel) and the total ERK level (lower panel) by immunoblotting. (b) Inhibition of MBP phosphorylation by PD98059 in the lysates from HBx DNA and insulin-injected mouse liver. Kinase reactions were conducted with the corresponding lysates (upper panel). Equal levels of MBP (CB staining) in all reactions are shown in the middle panel, essentially by SDS-PAGE analysis and Western blotting, as described in the text. (c) Fold activation of MBP phosphorylation. (d) Evaluation of the presence of HBx transcripts (upper panel) and the  $\beta$ -actin mRNA profile (lower panel) in the liver samples injected with HBx DNA. + and - represent the presence and absence of PD98059, respectively.

a result of the introduction of the MEK inhibitor (Fig. 4a and b, lower panels). Such inhibition by PD98059 provides pharmacological evidence that HBx specifically stimulates ERKs in vivo.

**Enhanced and sustained activation of ERKs in the HBx-expressing hepatocytes.** Activation of the ERK cascade has been well implicated in cell proliferation and differentiation. However, constitutive activation of this pathway has been re-

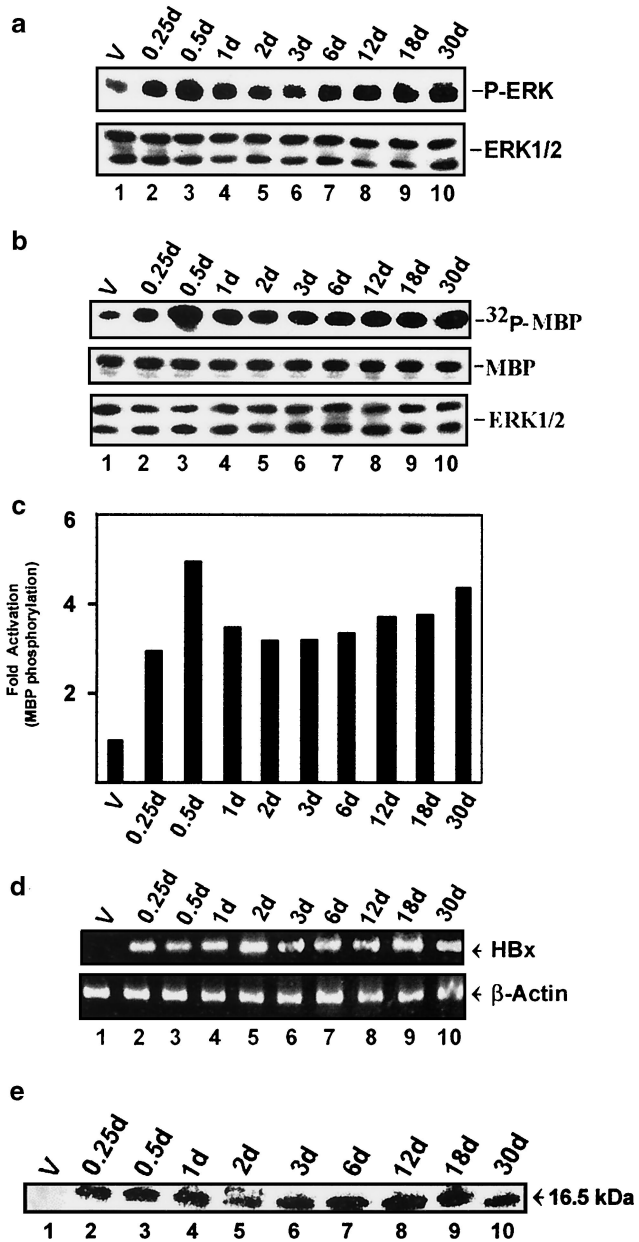


FIG. 5. Kinetics of ERK activation by HBx. (a) Extent of phosphorylation of ERKs (upper panel) and total ERK level (lower panel) in the hepatocyte lysates made from mice livers at different time points following a single injection of either virosomal HBx DNA or pSG5 vector. d, days. (b) MBP phosphorylation levels (upper panel), MBP levels (middle panel), and total ERK status (lower panel) in the same lysates. (c) Fold activation of MBP phosphorylation. (d) Tissue samples taken from all the time points were evaluated for the presence of HBx (upper panel) and  $\beta$ -actin mRNA transcripts (lower panel). (e) Western blot analysis of HBx protein following immunoprecipitation with anti-HBx monoclonal antibody (B-8/2/8) from liver cytosolic extracts. V, cell lysates from mice sacrificed 30 days after injection of the virosomal pSG5 vector.

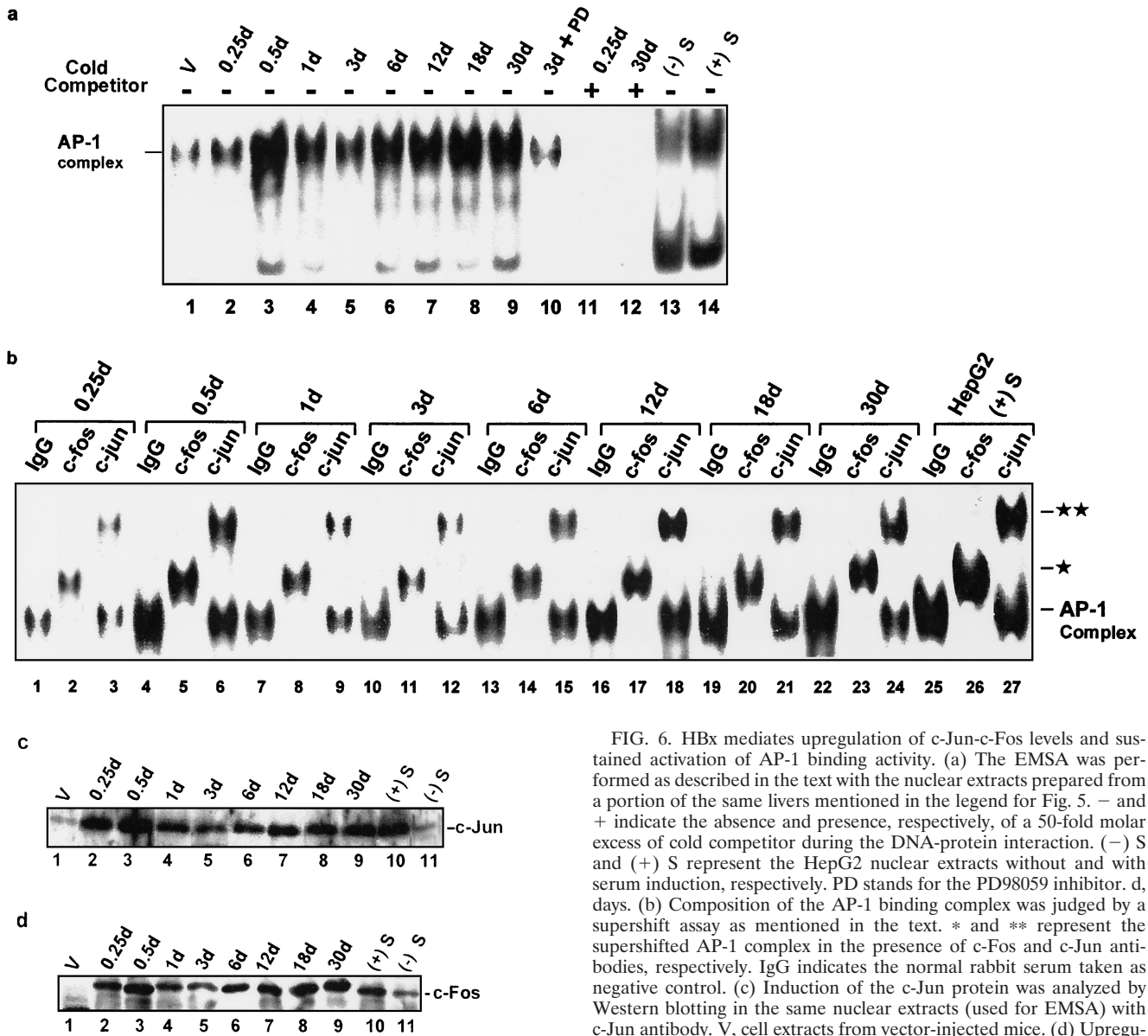


FIG. 6. HBx mediates upregulation of c-Jun-c-Fos levels and sustained activation of AP-1 binding activity. (a) The EMSA was performed as described in the text with the nuclear extracts prepared from a portion of the same livers mentioned in the legend for Fig. 5. - and + indicate the absence and presence, respectively, of a 50-fold molar excess of cold competitor during the DNA-protein interaction. (-) S and (+) S represent the HepG2 nuclear extracts without and with serum induction, respectively. PD stands for the PD98059 inhibitor. d, days. (b) Composition of the AP-1 binding complex was judged by a supershift assay as mentioned in the text. \* and \*\* represent the supershifted AP-1 complex in the presence of c-Fos and c-Jun antibodies, respectively. IgG indicates the normal rabbit serum taken as negative control. (c) Induction of the c-Jun protein was analyzed by Western blotting in the same nuclear extracts (used for EMSA) with c-Jun antibody. V, cell extracts from vector-injected mice. (d) Upregulation of the c-Fos protein was analyzed independently in the same nuclear extracts with c-Fos antibody. (+) S and (-) S, HepG2 extracts as used in panel a.

ported as one of the key reasons for the induction of a transformed phenotype by many oncogenes (34, 44, 45). Therefore, to explore the possibility of a similar aberrant activation scenario *in vivo* induced by HBx, hepatocyte lysates taken at progressive time points after the introduction of the HBx gene were examined for ERK activation using both the anti-phospho-ERK antibody assay (Fig. 5a) and the *in vitro* MBP kinase assay (Fig. 5b). Both the assays indicated significant upregulation of P-ERK and <sup>32</sup>P-MBP levels (three- to fivefold over that of the negative controls [Fig. 5b, upper panel, lanes 1 to 10, and Fig. 5c]). Such activation was apparent as early as 0.25 day (lane 2) and peaked at 0.5 day (lane 3), and strikingly, it remained elevated (up to threefold over the control) up to 30 days (the last time point studied) (lanes 4 to 10). In contrast, no significant increase in the steady-state levels of total ERK1/2 was evident during such an extended period of HBx expression

(Fig. 5a and b, lower panels). The RT-PCR profile and Western blot analysis from liver tissues showed a continued expression of the HBx gene till 30 days (Fig. 5d, upper panel, and e, lanes, 2 to 10). Therefore, expression of HBx *in vivo* leads to the activation of the ERK pathway, as observed in the case of oncogene-mediated sustained ERK activation (45).

**Persistent activation of AP-1 in HBx-expressing hepatocytes.** Activation of the MAPK cascade leads to the induction of AP-1 transcription factors and is generally implicated in proliferation and tumorigenesis (3, 26, 62, 67). Since in this study, HBx persistently activated ERKs, we next tested if the AP-1 binding activity was stimulated and maintained by HBx amidst the natural hepatocyte environment. To begin with, an EMSA was carried out using equal amounts of nuclear extracts

and the end-labeled AP-1 probe (Fig. 6a). HBx protein expression resulted in a sharp increase in AP-1 binding activity as early as 0.25 day following HBx gene administration, which reached the maximum at 0.5 day and remained elevated for up to 30 days (Fig. 6a, lanes 2 to 9). It is worth mentioning that liver samples used here are the same that were used for the ERK assay as described in the legends for Fig. 4 and 5. An excess of unlabeled AP-1 sequence effectively competed the protein-DNA complex (lanes 11 and 12), confirming the specificity of AP-1 binding. Furthermore, inhibition of AP-1 binding activity by PD98059 revealed the role of ERK in HBx-induced AP-1 activation (lane 10). Mice injected with vector DNA showed a basal level of DNA binding activity and served as a negative control (lane 1). Nuclear extracts were prepared from serum-starved and serum-stimulated HepG2 cells and used as negative and positive controls, respectively, as a measure of induction of AP-1 binding activity (lanes 13 and 14). To assess the composition of AP-1 binding complex, a supershift assay was also performed. Addition to nuclear extracts of antibody to c-Jun and c-Fos but not IgG resulted in supershifted complexes. Collectively, these results indicate that HBx expression also leads to a sustained increase in AP-1 binding activity comprised of the c-Jun and c-Fos heterodimer (Fig. 6b). To account for the persistent appearance of c-Jun and c-Fos proteins in the AP-1 complex, Western blots of the same nuclear extracts were performed using antibodies to c-Jun and c-Fos. Figure 6c and d show a significant increase in both c-Jun and c-Fos levels over that of the vector, suggesting that the increase of AP-1 binding activity occurs by an increase in *de novo* synthesis of c-Jun and c-Fos proteins.

**Induction of c-Jun levels: a consequence of prolonged activation of c-Jun N-terminal kinases (JNKs) by HBx.** Recent studies have provided evidence that JNKs are activated independently of ERKs and that following mitogenic stimuli, c-Jun acts as a downstream target of JNK activation (17, 46, 47, 49, 52, 58). Therefore, to determine whether JNK has any role in mediating the effect of HBx expression, we critically examined the levels of the phosphorylated form of JNKs (P-JNKs) and *vis-à-vis* the total JNKs in the HBx-transfected hepatocyte extracts (Fig. 7). A sharp increase in the phospho-JNK-specific bands, similar in pattern to HBx-induced ERK activation (Fig. 5), was observed in the hepatocyte lysates positive for HBx expression for a period from 0.25 to 30 days (Fig. 7, lanes 4 to 11). As observed in the case of ERKs, the total level of JNKs in all the time points tested remained unaltered in the presence of HBx transgene products (Fig. 7, lower panel).

**Long-term HBx protein expression: an outcome of integration of DNA in the chromosomes of hepatocytes.** To account for the sustained signal observed, we examined for the presence of HBx protein in the hepatocytes of liver sections 30 days postinjection by immunohistochemistry (Fig. 8a). As is evident from panel 1, nearly 70% of the hepatocytes sustained HBx gene expression. In an attempt to corroborate this observation, we carried out a systematic analysis on the status of the delivered HBx DNA in the host genome. Southern analysis (Fig. 8b) revealed the integration of the HBx gene in the chromosomal DNA from 3 days onward (till 30 days, the last time point taken).

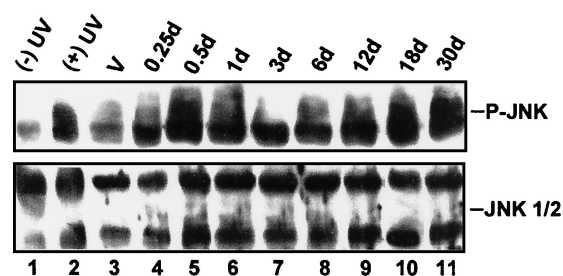


FIG. 7. Induction of JNKs by HBx. Equal amount (5  $\mu$ g) of the same hepatocyte cell extracts mentioned in the legend for Fig. 5 were subjected to Western blotting, and bands corresponding to activated JNKs (P-JNK, upper panel) and total JNKs (JNK1/2, lower panel) were detected. (-) UV and (+) UV represent total cell extracts from unirradiated and irradiated 293 cells as the negative and positive control, respectively. V, cell extracts from mice sacrificed after 30 days of virosomal vector DNA injection; d, days.

## DISCUSSION

In the present study, we expressed HBx in its physiological environment of hepatocytes in whole animal and analyzed its role as a transactivator in influencing mitogenic signaling pathways. Importantly, we demonstrate that HBx has the potential to activate MAPKs and AP-1 in a sustained manner resembling the mechanism of action of oncogenic stimulus.

HBx is implicated in HBV-mediated hepatocarcinogenesis, and its oncogenic potential is demonstrated with the CD1 strain of mouse (29) and cultured cell lines FMH202, AML12, and REV2 (2). Although the precise role of HBx in HCC remains unclear, HBx transactivation function in modulation of the signal transduction pathways could be envisaged as one of the possible mechanisms for carcinogenesis (4). The relevance of HBx-induced signaling cascades in cellular transformation could not be assessed by the available systems, as they fail to reproduce the normal hepatocyte environment due to constraints imposed by an altered genetic background. For example, the mouse CD1 strain is characterized by a high incidence of spontaneous cancer (22), while the immortalized cell lines have the insertion of certain transgenes, such as those for the epidermal growth factor receptor in AML12 (50), SV40 large T in FMH202 (21), and E1A in REV2 (20), that alter the normal physiological functions of the hepatocyte. Nevertheless, the ability of HBx to activate MAPK pathways is shown in transformed cell lines (9). However, recently Tarn et al. demonstrated that HBx-dependent induction of signaling cascades and the expression of their downstream immediate-early gene products c-Fos and ATF3 differed in transformed and non-transformed hepatic cell lines, in terms of both magnitude and duration (60). Furthermore, because of inherent problems, such as short life span, dedifferentiation, and difficulty in transfection, primary hepatocytes are not suitable for studying HBx-transactivating potential in oncogenesis (2, 14, 21). Such studies therefore implicate the prerequisite of the normal, nontransformed, and differentiated environment of hepatocytes and foster the importance of *in vivo* studies for functional analysis of HBx. However, none of the putative roles of HBx in the signaling cascades has been proven using animals *in vivo*. For these reasons it is especially important to study the acute effect of HBx expression in intact livers.



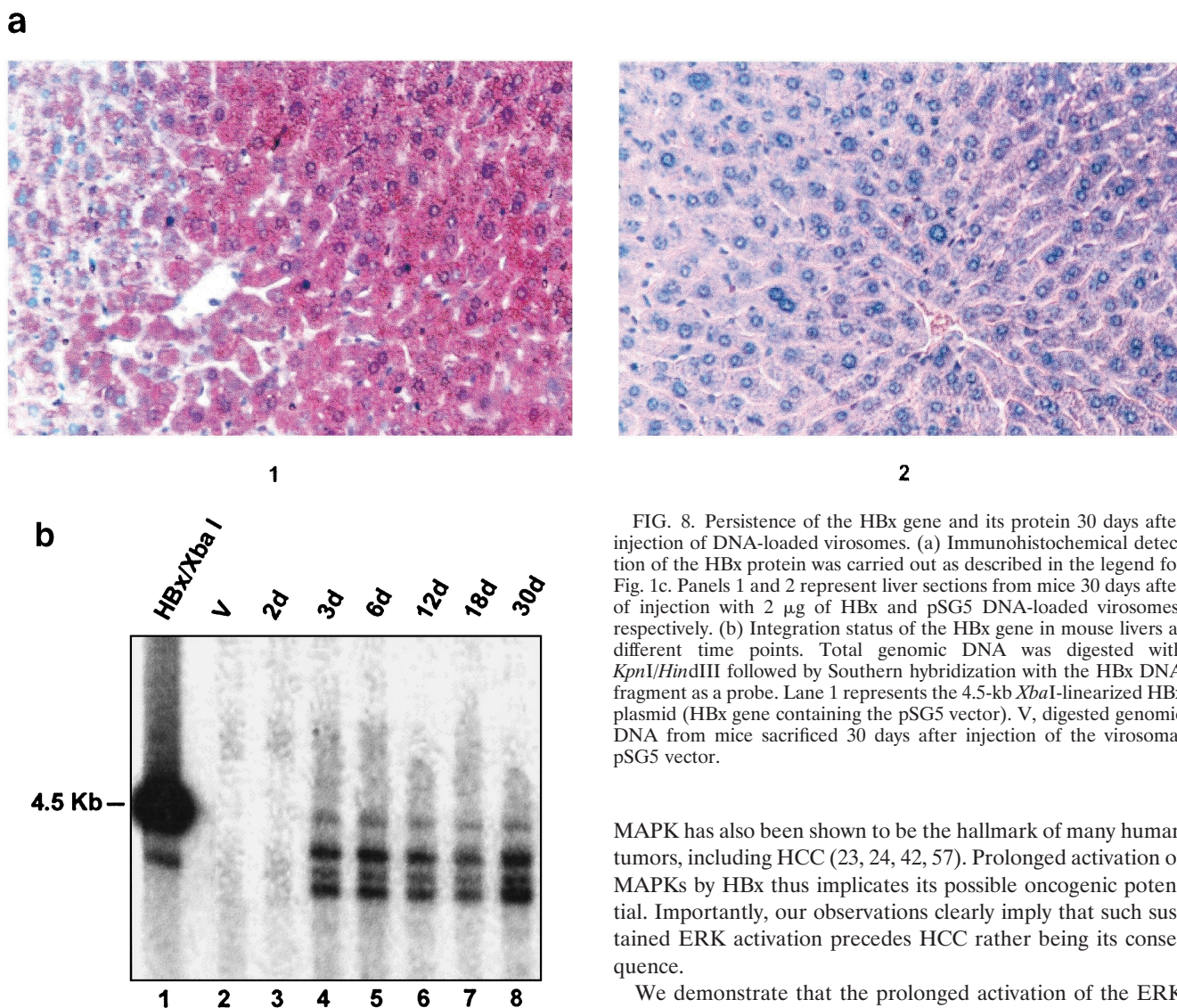


FIG. 8. Persistence of the HBx gene and its protein 30 days after injection of DNA-loaded virosomes. (a) Immunohistochemical detection of the HBx protein was carried out as described in the legend for Fig. 1c. Panels 1 and 2 represent liver sections from mice 30 days after of injection with 2  $\mu$ g of HBx and pSG5 DNA-loaded virosomes, respectively. (b) Integration status of the HBx gene in mouse livers at different time points. Total genomic DNA was digested with *KpnI/HindIII* followed by Southern hybridization with the HBx DNA fragment as a probe. Lane 1 represents the 4.5-kb *XbaI*-linearized HBx plasmid (HBx gene containing the pSG5 vector). V, digested genomic DNA from mice sacrificed 30 days after injection of the virosomal pSG5 vector.

HBx-expressing hepatocytes displayed an activation of ERK1/2 that was fourfold that of the negative controls and validated the *in vitro* observations of ERK activation by HBx (9) but contradicted the findings of Bergametti et al. in CCL-13 cell lines (12). The specificity of stimulation of ERK by HBx was further confirmed by the effect of a cytostatic drug, PD98059, that is a specific and efficient inhibitor for MEK (1), also suggesting that HBx-induced ERK activation requires MEK. ERK activation was induced rapidly within hours after the introduction of HBx and was prolonged over a period of 30 days. This sustained activation of ERK1/2 is to be contrasted with the transient activation seen in response to various growth factors where activity is maximal in 5 min and subsides rapidly within 30 to 60 min (31). The constitutive activation of ERKs by HBx appears to be similar to what has been observed with many oncogenes (15, 44, 45, 65). Previous studies show that transformation by oncogene products like Ras, Src, and Abl accompanies the constitutive activation of MAPK signaling pathways (44, 45, 65). Aberrant and inappropriate activation of

MAPK has also been shown to be the hallmark of many human tumors, including HCC (23, 24, 42, 57). Prolonged activation of MAPKs by HBx thus implicates its possible oncogenic potential. Importantly, our observations clearly imply that such sustained ERK activation precedes HCC rather being its consequence.

We demonstrate that the prolonged activation of the ERK activity by HBx expression is also accompanied by the activation of JNKs, which constitute another important member of the MAPK family primarily implicated in stress response. The activation of JNKs in the intact liver by HBx is in agreement with the similar observations made by Benn et al. with cultured hepatocytes (11). ERKs and JNKs are associated with divergent biological responses. While ERKs are linked to growth and differentiation, the JNK pathway induces apoptosis (17). Our observations that the ERK and JNK pathways are simultaneously activated by HBx are, however, not unusual in the context of numerous studies which demonstrate that activation of both the ERK and JNK signaling pathways is required to trigger a full spectrum of phenotypic traits associated with cellular transformation and oncogenesis (17, 63). In addition, it is known that the JNK-dependent apoptotic signaling pathway can be blocked by activation of survival signaling pathways, such as those of ERK, NF- $\kappa$ B, and Akt/PKB (17). A recent study paradoxically shows that JNKs act synergistically with ERKs to enhance a proliferative effect by phosphorylating c-Jun and protecting cells from apoptosis (64). Therefore, JNK pathway functions within the overall context of the state of

activation of other signaling pathways. In the light of this evidence we propose that HBx-induced JNK activation acts in accord with ERK activation, having a coherent effect on cell proliferation.

Activated ERKs and JNKs mediate their effects by translocating into the nucleus, phosphorylating various transcription factors, and thus reprogramming gene expression (3, 26, 17). Members of the AP-1 family of transcription factors are substrates for ERK/JNK activities and are the primary mediators of mitogenic stimulation (3, 26, 62, 67). Our results evidenced increased binding activity of AP-1 that precisely followed the pattern of ERK/JNK activation. Previous studies show a role of AP-1 comprised of the c-Jun-c-Fos heterodimer in cell proliferation (35, 62, 67). Recent studies have documented that Jun can promote cyclin gene expression and cell cycle progression (8). Note that in HepG2 cells in culture, inhibitory AP-1 complexes composed of Jun-Fra heterodimers, induced by BHQ, antagonize the transcriptional effects of the tumor promoter tetradecanoyl phorbol acetate, which are mediated by Jun-Fos heterodimers (66). Therefore, an increase in c-Jun and c-Fos heterodimers comprising the AP-1 complex suggests that most of the effect of HBx is in inducing stimulatory AP-1 complexes. However, our results are in contrast to the *in vitro* results found by Benn et al., where the Jun-Fos heterodimer was replaced by a Jun homodimer after 24 h (11). On the other hand, the findings of Kekulé et al. (27) that both Jun and Fos are needed to mediate AP-1 activation by HBx are authenticated by our *in vivo* results. Our observations on increased levels of c-Fos protein in HBx-expressing liver cells support the findings of Avantaggiati et al. with AML12 cells *in vitro* (5), although they are in discordance with the transient c-Fos levels observed by Benn et al. in Chang and HepG2 cell lines (11). The discrepancies observed with cultured cells prove the limited value of *in vitro* systems for such functional analysis and highlight the importance of our *in vivo* findings. Moreover, the increased c-Jun and c-Fos levels observed in our study might have relevance for hepatocyte transformation in the light of a recent report on the high endogenous levels of AP-1 in oncogenic activity compared to that needed for normal growth (62). Studies by Ito et al. on elevated MAPK activity and c-Fos levels in human HCC lend further support to our speculation (24). Notably, we observed a transient decline in both Jun and Fos levels during days 1 to 6, followed by another burst of Jun and Fos induction. It is anticipated that during the first phase of enhanced AP-1 activity, a distinct gene expression program is activated which subsequently stabilizes the enhanced AP-1 activity and possibly leads to cellular transformation.

Although our study suggests a potential role of HBx-induced signaling cascades in carcinogenesis, it does not preclude the involvement of additional mechanisms in such a process. It might be speculated that HBx behaves as a weak oncogene that alone is not sufficient but requires other cooperating oncogenic alterations, such as inactivation of p53 or overexpression of c-myc or cyclin D1, for malignant transformation. While HBV-associated HCC is a multistep process, it is likely that HBx alone may not lead to tumor formation but rather may contribute by deregulating cellular processes that eventually lead to liver cancer. Alternatively, the X protein might play a decisive role in hepatocarcinogenesis (till the precancerous phase only) but may not be necessary to maintain the tumor pheno-

type (16, 28, 56). In summary, we demonstrate that introduction of HBx in the adult mouse liver rapidly activates ERKs and JNKs and leads to an increase in AP-1 activity through the induction of the c-Fos and c-Jun proteins. The effect appears to be sustained, most likely because of the integration of the HBx gene into the host cell chromosome and its continued expression. The importance of our study lies in the fact that it describes the early cellular signaling events related to HBx-mediated carcinogenesis. The present report thus establishes for the first time a murine model for studying the molecular basis of HBV pathogenesis that can be used for further investigations on multistep process leading to HCC.

#### ACKNOWLEDGMENTS

We thank S. C. Basu, A. Puri, P. S. Chowdhury, K. Datta, P. K. Ghosh, S. Sopory, S. Panda, and S. Sinha for stimulating discussions and A. Datta, J. Haque, S. Saxena, and S. Sarkar for providing many useful reagents and constructive criticism. Help rendered by Anirudha Sengupta in performing immunohistochemical staining is gratefully acknowledged.

We are grateful to the Department of Biotechnology (DBT) (project no. BT/PRD660/PID/25/005/97) and Council of Scientific and Industrial Research (CSIR) (project no. 60(0019)/96/EMR-II), Government of India, for financial support. R.N. and S.S.J. thank CSIR for a research fellowship.

#### REFERENCES

- Alessi, D. R., A. Cuenda, P. Cohen, D. T. Dudley, and A. R. Saltiel. 1995. PD 098059 is a specific inhibitor of the activation of mitogen-activated protein kinase kinase *in vitro* and *in vivo*. *J. Biol. Chem.* **270**:27489–27494.
- Andrisani, O. M., and S. Barnabas. 1999. The transcriptional function of the hepatitis B virus X protein and its role in hepatocarcinogenesis. *Int. J. Oncol.* **15**:373–379.
- Angel, P., and M. Karin. 1991. The role of Jun, Fos and the AP-1 complex in cell-proliferation and transformation. *Biochim. Biophys. Acta* **1072**:129–157.
- Arbuthnot, P., A. Capovilla, and M. Kew. 2000. Putative role of hepatitis B virus X protein in hepatocarcinogenesis: effects on apoptosis, DNA repair, mitogen-activated protein kinases and JAK/STAT pathways. *J. Gastroenterol. Hepatol.* **15**:357–368.
- Avantaggiati, M. L., G. Natoli, C. Balsano, P. Chirillo, M. Artini, E. De Marzio, D. Collepardo, and M. Levrero. 1993. The hepatitis B virus (HBV) pX transactivates the *c-fos* promoter through multiple *cis*-acting elements. *Oncogene* **8**:1567–1574.
- Bagai, S., A. Puri, R. Blumenthal, and D. P. Sarkar. 1993. Hemagglutinin-neuraminidase enhances F protein-mediated membrane fusion of reconstituted Sendai virus envelopes with cells. *J. Virol.* **67**:3312–3318.
- Bagai, S., and D. P. Sarkar. 1994. Fusion-mediated microinjection of lysozyme into HepG2 cells through hemagglutinin neuraminidase-depleted Sendai virus envelopes. *J. Biol. Chem.* **269**:1966–1972.
- Bakiri, L., D. Lallemand, E. Bossy-Wetzel, and M. Yaniv. 2000. Cell cycle-dependent variations in c-Jun and JunB phosphorylation: a role in the control of cyclin D1 expression. *EMBO J.* **19**:2056–2068.
- Benn, J., and R. J. Schneider. 1995. Hepatitis B virus HBx protein deregulates cell-cycle checkpoint controls. *Proc. Natl. Acad. Sci. USA* **92**:11215–11219.
- Benn, J., and R. J. Schneider. 1994. Hepatitis B virus HBx protein activates Ras-GTP complex formation and establishes a Ras, Raf, MAP kinase signaling cascade. *Proc. Natl. Acad. Sci. USA* **91**:10350–10354.
- Benn, J., F. Su, M. Doria, and R. J. Schneider. 1996. Hepatitis B virus HBx protein induces transcription factor AP-1 by activation of extracellular signal-regulated and c-Jun N-terminal mitogen-activated protein kinases. *J. Virol.* **70**:4978–4985.
- Bergametti, F., S. Perigent, B. Luber, A. Benoit, P. Tiollais, A. Sarasin, and C. Transy. 1999. The proapoptotic effect of hepatitis B virus HBx protein correlates with its transactivation activity in stably transfected cell lines. *Oncogene* **18**:2860–2871.
- Boulton, T. G., S. H. Nye, D. J. Robbins, N. Y. Ip, E. Radziejewska, S. D. Morgenbesser, R. A. DePinho, N. Panayotatos, M. H. Cobb, and G. D. Yancopoulos. 1991. ERKs: a family of protein-serine/threonine kinases that are activated and tyrosine phosphorylated in response to insulin and NGF. *Cell* **65**:663–675.
- Caselmann, W. H. 1996. Trans-activation of cellular genes by hepatitis B virus proteins: a possible mechanism of hepatocarcinogenesis. *Adv. Virus Res.* **47**:253–302.

15. Cowley, S., H. Paterson, P. Kemp, and C. J. Marshall. 1994. Activation of MAP kinase kinase is necessary and sufficient for PC12 differentiation and for transformation of NIH 3T3 cells. *Cell* **77**:841–852.
16. Dandri, M., P. Schirmacher, and C. E. Rogler. 1996. Woodchuck hepatitis virus X protein is present in chronically infected woodchuck liver and woodchuck hepatocellular carcinomas which are permissive for viral replication. *J. Virol.* **70**:5246–5254.
17. Davis, R. J. 2000. Signal transduction by the JNK group of MAP kinases. *Cell* **103**:239–252.
18. Doria, M., N. Klein, R. Lucito, and R. J. Schneider. 1995. The hepatitis B virus HBx protein is a dual specificity cytoplasmic activator of Ras and nuclear activator of transcription factors. *EMBO J.* **14**:4747–4757.
19. Ganem, D., and H. E. Varmus. 1987. The molecular biology of the hepatitis B viruses. *Annu. Rev. Biochem.* **56**:651–693.
20. Gottlob, K., S. Pagano, M. Leverro, and A. Graessmann. 1998. Hepatitis B virus X protein transcription activation domains are neither required nor sufficient for cell transformation. *Cancer Res.* **58**:3566–3570.
21. Hohne, M., S. Schaefer, M. Seifer, M. A. Feitelson, D. Paul, and W. H. Gerlich. 1990. Malignant transformation of immortalized transgenic hepatocytes after transfection with hepatitis B virus DNA. *EMBO J.* **9**:1137–1145.
22. Homburger, F., A. B. Russfield, J. H. Weisburger, S. Lim, S. P. Chak, and E. K. Weisburger. 1975. Ageing changes in CD1 Ham/ICR mice treated under standard laboratory conditions. *J. Natl. Cancer Inst.* **55**:37–45.
23. Hoshino, R., Y. Chatani, T. Yamori, T. Tsuruo, H. Oka, O. Yoshida, Y. Shimada, S. Ari-i, H. Wada, F. Fujimoto, and M. Kohno. 1999. Constitutive activation of the 41-/43-kDa mitogen-activated protein kinase signaling pathway in human tumors. *Oncogene* **18**:813–822.
24. Ito, Y., Y. Sasaki, M. Horimoto, S. Wada, Y. Tanaka, A. Kasahara, T. Ueki, T. Hirano, H. Yamamoto, J. Fujimoto, E. Okamoto, N. Hayashi, and M. Hori. 1998. Activation of mitogen-activated protein kinases/extracellular signal-regulated kinases in human hepatocellular carcinoma. *Hepatology* **27**:951–958.
25. Jameel, S., A. Siddiqui, H. F. Maguire, and K. V. S. Rao. 1990. Hepatitis B virus X protein produced in *Escherichia coli* is biologically functional. *J. Virol.* **64**:3963–3966.
26. Karin, M. 1995. The regulation of AP-1 activity by mitogen-activated protein kinases. *J. Biol. Chem.* **270**:16483–16486.
27. Kekulé, A. S., U. Lauer, L. Weiss, B. Lubber, and P. H. Hofschneider. 1993. Hepatitis B virus transactivator HBx uses a tumor promoter signaling pathway. *Nature* **361**:742–745.
28. Kekulé, A. S., U. Lauer, M. Meyer, W. H. Caselmann, P. H. Hofschneider, and R. Koshy. 1990. The preS2/S region of integrated hepatitis B virus DNA encodes a transcriptional transactivator. *Nature* **343**:457–461.
29. Kim, C. M., K. Koike, I. Saito, T. Miyamura, and G. Jay. 1991. HBx gene of hepatitis B virus induces liver cancer in transgenic mice. *Nature* **351**:317–320.
30. Klein, N. P., and R. J. Schneider. 1997. Activation of Src family kinases by hepatitis B virus HBx protein and coupled signaling to Ras. *Mol. Cell. Biol.* **17**:6427–6436.
31. Kohno, M. 1985. Diverse mitogenic agents induce rapid phosphorylation of a common set of cellular proteins at tyrosine in quiescent mammalian cells. *J. Biol. Chem.* **260**:1771–1779.
32. Koike, K., and S. Takada. 1995. Biochemistry and functions of hepatitis B virus X protein. *Intervirolgy* **38**:89–99.
33. Koike, K., K. Moriya, H. Yotsuyanagi, S. Iino, and K. Kurokawa. 1994. Induction of cell cycle progression by hepatitis B virus HBx gene expression in quiescent mouse fibroblasts. *J. Clin. Investig.* **94**:44–49.
34. Kolch, W. 2000. Meaningful relationships: the regulation of the Ras/Raf/MEK/ERK pathway by protein interactions. *Biochem. J.* **351**:289–305.
35. Kovary, K., and R. Bravo. 1992. Existence of different Fos/Jun complexes during the G<sub>0</sub>-to-G<sub>1</sub> transition and during exponential growth in mouse fibroblasts: differential role of Fos proteins. *Mol. Cell. Biol.* **12**:5015–5023.
36. Krajcsi, P., and W. S. M. Wold. 1998. Viral proteins that regulate cellular signaling. *J. Gen. Virol.* **79**:1323–1335.
37. Kumar, V., N. Jaysuryan, and R. Kumar. 1996. A truncated mutant (residues 58-140) of the hepatitis B virus X protein retains transactivation function. *Proc. Natl. Acad. Sci. USA* **93**:5647–5652.
38. Lassar, A. B., J. N. Buskin, D. Lockshon, R. L. Davis, S. Apone, S. D. Hauschka, and H. Weintraub. 1991. Functional activity of myogenic HLH protein requires hetero-oligomerization with E12/E47 like protein in vivo. *Cell* **66**:305–315.
39. Lee, T., M. J. Finegold, R. Shen, J. L. DeMayo, S. L. C. Woo, and J. S. Butel. 1990. Hepatitis B virus transactivator X protein is not tumorigenic in transgenic mice. *J. Virol.* **64**:5939–5947.
40. Lee, Y. H., and Y. Yun. 1998. HBx protein of hepatitis B virus activates Jak1-STAT signaling. *J. Biol. Chem.* **273**:25510–25515.
41. Lewis, T. S., P. S. Shapiro, and N. G. Ahn. 1998. Signal transduction through MAP kinases cascades. *Adv. Cancer Res.* **74**:49–139.
42. Maemura, M., Y. Lino, Y. Koibuchi, T. Yokoe, and Y. Morishita. 1999. Mitogen-activated protein kinase cascade in breast cancer. *Oncology* **57**:(Suppl. 2):37–44.
43. Manna, S. K., C. Bhattacharya, S. K. Gupta, and A. K. Samanta. 1995. Regulation of interleukin-8 receptor expression in human polymorphonuclear neutrophils. *Mol. Immunol.* **32**:883–893.
44. Mansour, S. J., W. T. Matten, A. S. Hermann, J. M. Candia, S. Rong, K. Fukasawa, G. F. Vande Woude, and N. G. Ahn. 1994. Transformation of mammalian cells by constitutively active MAP kinase kinase. *Science* **265**:966–970.
45. McCormick, F. 1999. Signaling networks that cause cancer. *Trends Biochem. Sci.* **24**:M53–M56.
46. Minden, A., A. Lin, M. McMahon, C. Lange-Carter, B. Derijard, R. J. Davis, G. L. Johnson, and M. Karin. 1994. Differential activation of ERK and JNK mitogen-activated protein kinases by Raf-1 and MEKK. *Science* **266**:1719–1723.
47. Minden, A., A. Lin, T. Smeal, B. Derijard, M. Cobb, R. Davis, and M. Karin. 1994. c-Jun N-terminal phosphorylation correlates with activation of the JNK subgroup but not the ERK subgroup of mitogen-activated protein kinases. *Mol. Cell. Biol.* **14**:6683–6688.
48. Murakami, S. 1999. Hepatitis B virus X protein: structure, function and biology. *Intervirolgy* **42**:81–99.
49. Musti, A. M., M. Treier, and D. Bohmann. 1997. Reduced ubiquitin-dependent degradation of c-Jun after phosphorylation by MAP kinases. *Science* **275**:400–402.
50. Oguey, D., L. L. Dumenco, R. H. Pierce, and N. Fausto. 1996. Analysis of the tumorigenicity of the X gene of hepatitis B virus in a nontransformed hepatocyte cell line and the effects of cotransfection with a murine p53 mutant equivalent to human codon 249. *Hepatology* **24**:1024–1033.
51. Ostrowski, J., M. Woszczynski, P. Kowalczyk, L. Trzeciak, E. Hennig, and K. Bomsztyk. 2000. Treatment of mice with EGF and orthovanadate activates cytoplasmic and nuclear MAPK, p70S6k, and p90rsk in the liver. *J. Hepatol.* **32**:965–974.
52. Pulverer, B. J., J. M. Kryakis, J. Avrych, E. Nikolakakie, and J. Woodgett. 1991. Phosphorylation of c-Jun mediated by MAP kinases. *Nature (London)* **353**:670–674.
53. Ramani, K., Q. Hassan, B. Venkaiah, S. E. Hasnain, and D. P. Sarkar. 1998. Site-specific gene delivery in vivo through engineered Sendai viral envelopes. *Proc. Natl. Acad. Sci. USA* **95**:11886–11890.
54. Reinfenber, K., H. Wilts, J. Lohler, P. Nusser, R. Hanano, L. G. Guidotti, F. V. Chisari, and H. Schlicht. 1999. The hepatitis B virus X protein transactivates viral core gene expression in vivo. *J. Virol.* **73**:10399–10405.
55. Robinson, M. J., and M. H. Cobb. 1997. Mitogen-activated protein kinase pathways. *Curr. Opin. Cell Biol.* **9**:180–186.
- 55a. Sarkar, D. P. November 1997. U.S. patent 5,683,866.
56. Schluter, V., M. Meyer, P. H. Hofschneider, R. Koshy, and W. H. Caselmann. 1994. Integrated hepatitis B virus X and 3' truncated preS/S sequences derived from human hepatomas encode functionally active transactivators. *Oncogene* **9**:3335–3344.
57. Schmidt, C. M., I. H. McKillop, P. A. Cahill, and J. V. Sitzmann. 1997. Increased MAPK expression and activity in primary human hepatocellular carcinoma. *Biochem. Biophys. Res. Commun.* **236**:54–58.
58. Smeal, T., B. Binetruy, D. A. Mercola, M. Birrer, and M. Karin. 1991. Oncogenic and transcriptional cooperation with Ha-Ras requires phosphorylation of c-Jun on serines 63 and 73. *Nature* **354**:494–496.
59. Talarmin, H., C. Rescan, S. Cariou, D. Glaise, G. Zanninelli, M. Bilodeau, P. Loyer, C. Gueguen-Guillouzo, and G. Baffet. 1999. The mitogen-activated protein kinase/extracellular signal-regulated kinase cascade activation is a key signaling pathway involved in the regulation of G<sub>1</sub> phase progression in proliferating hepatocytes. *Mol. Cell. Biol.* **19**:6003–6011.
60. Tarn, C., M. L. Bilodeau, R. L. Hullinger, and O. M. Andrisani. 1999. Differential immediate early gene expression in conditional hepatitis B virus pX-transforming versus nontransforming hepatocyte cell lines. *J. Biol. Chem.* **274**:2327–2336.
61. Tiollais, P., C. Pourcel, and A. Dejean. 1985. The hepatitis B virus. *Nature* **317**:489–495.
62. Ui, M., T. Mizutani, M. Takada, T. Arai, T. Ito, M. Murakami, C. Koike, T. Watanabe, K. Yoshimatsu, and H. Iba. 2000. Endogenous AP-1 levels necessary for oncogenic activity are higher than those sufficient to support normal growth. *Biochem. Biophys. Res. Commun.* **278**:97–105.
63. Van Putten, V., Z. Refaat, C. Dessev, S. Blaine, M. Wick, L. Butterfield, S. Y. Han, L. E. Heasley, and R. A. Nemenoff. 2001. Induction of cytosolic phospholipase A2 by oncogenic Ras is mediated through the JNK and ERK pathways in rat epithelial cells. *J. Biol. Chem.* **276**:1226–1232.
64. Wisdom, R., R. S. Johnson, and C. Moore. 1999. c-Jun regulates cell cycle progression and apoptosis by distinct mechanisms. *EMBO J.* **18**:188–197.
65. Yamamoto, T., S. Taya, and K. Kaibuchi. 1999. Ras-induced transformation and signaling pathway. *J. Biochem.* **126**:799–803.
66. Yoshioka, K., T. Deng, M. Cavigelli, and M. Karin. 1995. Antitumor promotion by phenolic antioxidants: inhibition of AP-1 activity through induction of Fra expression. *Proc. Natl. Acad. Sci. USA* **92**:4972–4976.
67. Young, M. R., J. Li, M. Rincon, R. A. Flavell, B. K. Sathyanarayana, R. Hunziker, and N. Colburn. 1999. Transgenic mice demonstrate AP-1 (activator protein-1) transactivation is required for tumor promotion. *Proc. Natl. Acad. Sci. USA* **96**:9827–9832.